Journal of Materials Chemistry B

ROYAL SOCIETY OF CHEMISTRY

PAPER

View Article Online
View Journal | View Issue

Cite this: *J. Mater. Chem. B*, 2021, **9**, 1288

A novel cyanoacrylate-based matrix excipient in HPMCP capsules forms a sustained intestinal delivery system for orally administered drugs with enhanced absorption efficiency†

Liya Song,[ab] Pengfei Chen,[c] Jin Yu,[d] Xiaolu Han,[a] Yabing Hua,[a] Shan Liu,[e] Bo Pang,[f] Jing Gao,[a] Jiahua Ma*[b] and Liang Xu *[a]

Received 4th November 2020,
Accepted 22nd December 2020

DOI: 10.1039/d0tb02606a

rsc.li/materials-b

Patients prefer oral drug delivery due to its convenience and noninvasiveness. Nevertheless, a multitude of potentially clinically important drugs will not reach the market or achieve their full potential, due to their low bioavailability and instability in gastric acid. In this study, a novel oral drug delivery system based on poly-cyanoacrylate [a polymer of 2-(2-methoxyethoxy)ethyl-2-cyanoacrylate (MECA)] and hydroxypropyl methylcellulose phthalate (HPMCP) was developed and shown to permit intestinal targeting and sustained drug release. Aspirin [acetylsalicylic acid (ASA)] was selected as a model drug for atherosclerosis treatment. It was physically dissolved in liquid MECA, and the ASA–MECA matrix was then polymerized into a solid drug-loading depot in an HPMCP shell. The delivery of the drug depot in the intestine was achieved with the HPMCP shell; then the polymerized MECA (polyMECA) provided sustained drug release. The polyMECA excipient was not absorbed by the intestine due to its high molecular weight; a fluorescein-labeled assay indicated that it was excreted completely in feces after drug release. The formulation, ASA–polyMECA–HPMCP, showed good intestinal targeting and sustained drug release *in vitro* and *in vivo*. Pharmacokinetic studies indicated that this formulation improved the bioavailability of ASA relative to commercially available controls. ASA–polyMECA–HPMCP showed desirable anti-atherosclerosis efficacy in a rabbit model, with significant enhancement of atheromatous lesion stability. Biosafety tests proved the low toxicity of ASA–polyMECA–HPMCP and the polyMECA matrix. We believe that this work has provided a practical and biocompatible system for sustained intestinal drug delivery that can be applied broadly with various drugs for specific therapeutic aims.

Introduction

Patients prefer the oral administration of pharmaceutical agents because of its convenience and the avoidance of painful procedures, among other reasons.[1,2] However, many hurdles are encountered with oral administration, such as the low bioavailability of agents due to degradation in the stomach and gastrointestinal irritation, especially at high dosages.[3–6] Intestine-targeting formulations for oral administration have attracted increasing attention in recent years; they have been developed with the aims of improving the treatment efficiency for local intestinal diseases (*e.g.*, colorectal infections and colorectal cancer), providing an alternative route for the systemic absorption of conventional and labile drugs, and reducing gastric stimulation and side effects.[7,8]

The use of polymeric materials is a valuable route to meet the challenges of drug storage and delivery.[9–11] Several natural and synthetic polymers, such as chitosan, pectin, and ethylcellulose, have been explored as excipients in small intestine- and colon-targeting formulations.[12–15] However, several are limited by their restricted adaptivity, low bioavailability, and/or complicated preparation, and commercially available materials for intestine or colon targeting still lack diversity. The development of new strategies and biomaterials

[a] *State Key Laboratory of Toxicology and Medical Countermeasures, Beijing Institute of Pharmacology and Toxicology, Beijing, China. E-mail: xuliang24998@yahoo.com*
[b] *School of Life Science and Engineering, Southwest University of Science and Technology, Mianyang 621010, China*
[c] *Department of Cardiology, the 6th Medical Center, Chinese PLA General Hospital, Beijing 100853, China*
[d] *Department of Neurology (the First Medical Center), Chinese PLA General Hospital, Beijing 100853, China*
[e] *Pathology Department of PLA Rocket Force Characteristic Medical Center, Beijing 100085, China*
[f] *Clinical Laboratory, Guanganmen Hospital, China Academy of Chinese Medical Science, Beijing 100053, China*

† Electronic supplementary information (ESI) available. See DOI: 10.1039/d0tb02606a

for intestine-targeting oral drug delivery (ITODD) systems remains essential.

Atherosclerosis is the leading cause for many fatal cardiovascular and cerebrovascular diseases.[16,17] Accumulating evidence shows that atherosclerosis is caused not only by the accumulation of lipids in arterial walls, but also as a chronic inflammatory disease in response to vascular injury.[18] Extensive research has explored the targeting of inflammation to prevent the progression of atherosclerosis.[19–22] Aspirin [acetylsalicylic acid (ASA)], a conventional anti-platelet and anti-inflammatory agent used widely in clinical practice, plays therapeutic and preventive roles for atherosclerosis *via* the inhibition of platelet adhesion and aggregation, and the interruption of several steps in the inflammatory process associated with atherogenesis.[23–28] However, the decomposition of ASA in acidic environments and the rapid and extensive absorption of this agent in the upper intestinal tract can lead to severe side effects, such as gastrointestinal bleeding, ultimately leading to ASA intolerance in some patients.[29–31] Thus, the targeting of the intestinal region and extension of the drug's release time would improve the therapeutic effect of ASA for atherosclerosis.

In this study, a novel sustained ITODD system for the treatment of atherosclerosis, with ASA loaded as the model drug, was assessed. In particular, poly-cyanoacrylate (PCA) was used as a novel drug matrix excipient, filled in a capsule shell made of hydroxypropyl methyl cellulose phthalate (HPMCP). The HPMCP coating is pH sensitive. It could withstand the low pH in the stomach and will degrade in the neutral pH of the intestine,[32,33] which ensures that ASA can pass through the stomach completely and be released from the ASA–PCA complex depot in intestine. After drug release, the inert pharmacological polymer PCA is meant to be excreted directly, as it cannot be absorbed by the intestinal tract due to its high molecular weight. To our knowledge, this report is the first to describe the use of cyanoacrylate (CA) as a matrix excipient for oral drug delivery.

CA has well-known applications in the construction of medical adhesives and nanocarriers.[34–36] Its liquid monomers polymerize into a solid under certain conditions, providing opportunities for the direct dissolution of organic drugs by liquid CA and the formation of drug-loading depots of any desired shape and for any dose. However, *n*-butyl cyanoacrylate [BCA; Fig. 1(a)], the most commonly used CA polymer, is very hydrophobic and micromorphologically compact; thus, polyBCA is not an optimal material for the construction of drug-release depots.[37] To overcome these limitations, 2-(2-methoxyethoxy)-ethyl-2-cyanoacrylate [MECA; Fig. 1(b)], an alkoxy-modified CA monomer with better hydrophilicity, was used in this work for depot polymerization.

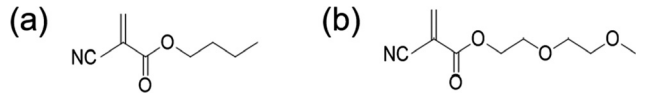

Fig. 1 Chemical structures of (a) *n*-butyl cyanoacrylate and (b) 2-(2-methoxyethoxy)ethyl 2-cyanoacrylate.

Table 1 CA compositions of the ASA–polyCA–HPMCP formulations

Sample	CA monomer composition	CA monomer wt%
ASA–polyBCA–HPMCP	BCA	—
ASA–polyMECA–HPMCP	MECA	—
ASA–polyBCA/MECA–HPMCP	BCA/MECA	50/50

Results and discussion

Monomers and ASA–polyCA–HPMCP formulations

Two CA monomers, BCA and MECA, were synthesized with high purity, as confirmed by proton nuclear magnetic resonance (^{1}H-NMR; Fig. S1, ESI†) and gas chromatography (99.1% for BCA, and 95.4% for MECA). MECA exhibited less polymer film formation and a smaller contact angle, confirming that its hydrophilicity was superior to that of BCA (Fig. S2 and Table S1, ESI†). Samples containing BCA and MECA (50/50, wt%) yielded intermediate results.

Three ASA–polyCA–HPMCP formulations with different CA compositions were prepared (Table 1). ASA (5%) dissolved readily, reaching a transparent liquid state, in the CA monomers. After maintenance at 80 °C for 24 h, the liquid ASA–CA complex had formed a solid depot. A ^{1}H-NMR assay confirmed the complete polymerization of the CA monomers, with the shifting of peaks at 7.05 and 6.62 ppm, corresponding to the olefinic double-bond protons, to 2.64 ppm (Fig. S3, ESI†). This liquid–solid transformational property of the drug-loading matrix leads to easy filling of shells molded into any shape with individualized doses.

Dispersion of ASA in the polyCA depot

^{1}H-NMR, ultraviolet (UV), and high-performance liquid chromatography (HPLC) assays were used to characterize ASA dispersion in the polyCA depot. Taking the ASA–polyMECA group as an example, the typical spectral peaks of ASA were detected in ^{1}H-NMR spectra obtained before and after MECA polymerization (Fig. S3, ESI†) and the UV absorption peak of ASA remained at 276 nm, as for free ASA [Fig. 2(a)]. HPLC showed the characteristic peaks of ASA in sample extracts [Fig. 2(b)], and randomly sampled depots had similar integral areas. These results indicate that ASA was physically and homogeneously dispersed in the polyMECA depot, with no chemical reaction occurring between these components. Homogeneous physical

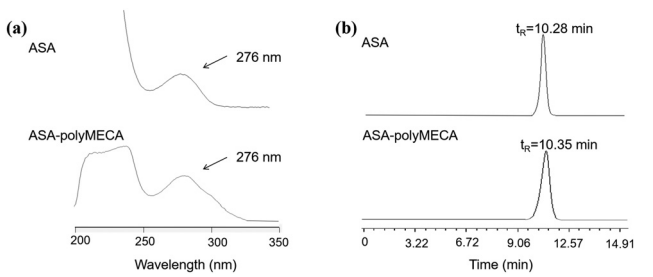

Fig. 2 (a) UV assay results and (b) HPLC chromatograms of ASA alone and ASA–polyMECA phosphate-buffered saline extract.

dispersion is of great significance, as it permits the adjustment of the drug dose *via* alteration of the volume of liquid used.

ASA release from the ASA–polyCA–HPMCP formulation *in vitro*

In an *in vitro* assay, the efficiency of ASA (5%, ASA in MECA) release from the ASA–polyCA–HPMCP formulation was evaluated under different pH conditions corresponding to the gastric (HCl, pH 1.2) and intestinal media (PBS, pH 6.8) at 37 °C (Fig. 3). As ASA partially and rapidly degrades to salicylic acid (SA) in phosphate-buffered saline (PBS) solution, the amount of ASA released was calculated by determining the total concentrations of free SA and ASA.[38,39] The ASA and SA peaks were well separated under the test conditions (Fig. S4, ESI†).

All three groups showed a limited drug release at pH 1.2 for the first 2 h, indicating that HPMCP provided reliable protection from gastric fluid. At pH 6.8, the outer layer of the capsule became degraded and corroded, and ASA–polyMECA–HPMCP samples showed a good sustained drug release profile, with approximately 90.65% of ASA released within 24 h. In contrast, ASA–polyBCA–HPMCP samples released little ASA in simulated intestinal fluid. ASA–polyBCA/MECA–HPMCP samples had a slightly higher ASA release rate (9.64%) than did ASA–polyBCA–HPMCP samples. Moreover, a control of ASA–HPMCP without any polymer depot showed burst release within 1 h after placing in pH 6.8. These results indicate that the CA formulation affected the ASA release behavior. The higher drug release rate in the ASA–polyMECA–HPMCP group may be attributable to the superior hydrophilicity of polyMECA relative to polyBCA. The increase in drug release with the addition of polyMECA in the ASA–polyBCA/MECA–HPMCP group indicates that drug release can be adjusted according to specific needs.

Fig. 4 shows the drug release with ASA–polyMECA–HPMCP (drug loading content is 5%, ASA in MECA) samples and two commercial products. Aspirin enteric capsules (ASA-ECs) showed little (2.79%) ASA release in simulated gastric fluid, and burst when placed in simulated small-intestinal fluid (98.76% release at 45 min). Aspirin enteric-coated sustained-release tablets (ASA-ETs) released little (5.61%) ASA at pH 1.2 and showed sustained release at pH 6.8 (98.42% within 8 h). ASA–polyMECA–HPMCP samples showed no ASA release in simulated gastric fluid and had a slower drug release rate than did commercial ASA-ETs (85.16% within 14 h, 90.65% within 24 h).

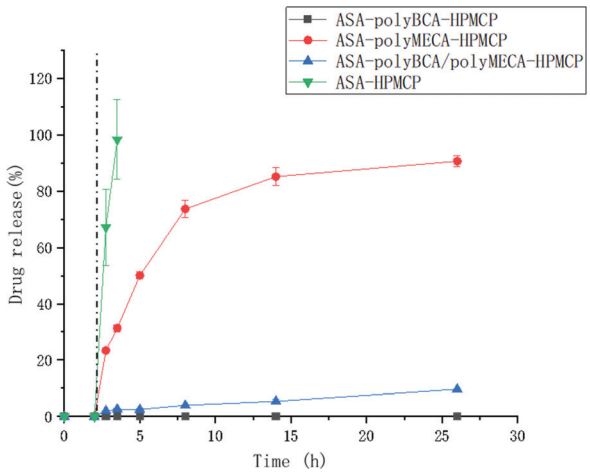

Fig. 3 Drug release curves. The dashed line represents the change of medium pH from 1.2 to 6.8. Data are means ± SDs (n = 3).

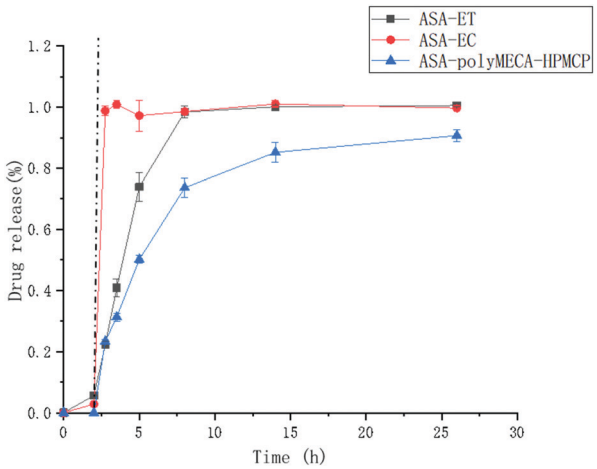

Fig. 4 Release profiles of ASA–polyMECA–HPMCP, ASA-ETs, and ASA-ECs in different media. The dashed line represents the change of medium pH from 1.2 to 6.8. Data are means ± SDs (n = 3).

ASA–polyMECA–HPMCP was chosen as the preferred formulation, given its appropriate drug release rate. Its drug release properties under different drug loading rates and matrix volumes were investigated further. Samples with the same polyMECA volumes (200 μL) but different drug loading rates (5%, 10%, and 15%) produced similar ASA release curves [Fig. S5(a), ESI†]. Those with the same drug loading rate (5%) but different polyMECA volumes (50, 100, and 200 μL) also showed parallel tendencies, although those containing 200 μL polyMECA had a slightly slower release rate [Fig. S5(b), ESI†]. This difference may be explained by the larger surface area of samples with less vehicle than of those with a larger volume contained in the same capsule shell. Moreover, Fig. S6 (ESI†) indicated that the molecular weight of polyMECA had little influence on ASA release.

The underlying interactions for drug releasing from depot include drug diffusion, depot erosion and degradation. To determine the mechanism of ASA release from the ASA–polyMECA complex in simulated intestinal fluid, the n parameter of the Korsmeyer–Peppas model ($\ln M_t/M_\infty = n \ln t + \ln k$) was computed ($R^2$ = 0.939). This value was 0.42, indicating that the release pattern could be characterized as a Fickian transport mechanism (in which the diffusion flux is proportional to the concentration gradient);[40,41] thus, diffusion was the principal release mechanism. The moderate hydrophilicity of polyMECA could provide water molecules gradually penetrating into the polymer, resulting in a sustained drug release, neither too fast nor too slow.

In vivo pharmacokinetics of ASA

In an *in vivo* rabbit model, plasma concentrations of ASA–polyMECA–HPMCP reached their maximum after 4 h

Table 2 Pharmacokinetic data for the *in vivo* oral administration of ASA–polyMECA–HPMCP (18 and 24 mg kg^{-1} ASA), commercially available ASA-ECs (24 mg kg^{-1} ASA), and free ASA solution (24 mg kg^{-1} ASA)

Sample	T_{max} (h)	C_{max} (mg mL^{-1})	$AUC_{(0-24)}$ (h mg mL^{-1})
Free ASA solution	0.25	0.005 ± 0.002	0.015 ± 0.001
ASA-EC (24 mg kg^{-1})	1	0.019 ± 0.006	0.123 ± 0.061
ASA–polyMECA–HPMCP (24 mg kg^{-1})	4	0.021 ± 0.002	0.188 ± 0.025
ASA–polyMECA–HPMCP (18 mg kg^{-1})	4	0.016 ± 0.003	0.136 ± 0.016

(Table 2). In contrast, the maximum drug concentration in blood was reached within 1 h with ASA-ECs, and this concentration was reached immediately but was very low with free ASA, due to the instability of ASA in gastric acid (Fig. 5). Importantly, the bioavailability of ASA–polyMECA–HPMCP samples with 24 mg kg^{-1} ASA (drug loading content is 20%) was superior to that of ASA-ECs with the same ASA dosage. ASA–polyMECA–HPMCP had an area under curve (AUC) value of 0.188 h mg mL^{-1}, which was 1.5-fold greater than that of commercial ASA-ECs and 12.5 times greater than that of free ASA solution. Moreover, the AUC value for ASA–polyMECA–HPMCP samples with 18 mg kg^{-1} ASA (drug loading content is 15%) was higher (1.1 times) than that for ASA-ECs with 24 mg kg^{-1} ASA. The improved bioavailability of the novel drug delivery system provides the potential to reduce the drug dosage, and thereby drug-related side effects. In our work, the ASA release and absorption in the intestinal tract were related much more to the inner polyMECA depot than to the outer HPMCP layer, due to the solubility of HPMCP at pH 5.5 in the duodenum.[33] PolyMECA showed a weak, but definite, adhesive capability when smeared between two pieces of intestine (Table S2, ESI†). This potential bioadhesive property may be attributable mainly to alkoxy modification, and is related to hydrogen bonding, van der Waals force, and mechanical interaction. Thus, the ASA–polyMECA formulation could have a prolonged retention time, which aids drug absorption and transport in the intestinal tract, thereby improving drug bioavailability.

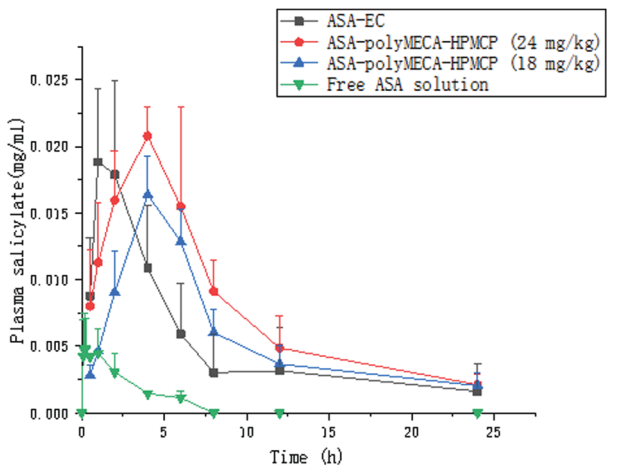

Fig. 5 Pharmacokinetics of 24 and 18 mg kg^{-1} ASA loaded with the polyMECA–HPMCP formulation, 24 mg kg^{-1} ASA in ECs, and free ASA solution (24 mg kg^{-1}) in New Zealand white rabbits. Data are means ± SDs (n = 9).

Excretion of polyMECA

Gel permeation chromatography (GPC) showed that the molecular weight of polyMECA in ASA–polyMECA–HPMCP samples exceeded 50 kDa (Fig. S7, ESI†), which exceeds the limit of glomerular filtration.

To intuitively observe its metabolism course *in vivo*, polyMECA was labeled with fluorescein isothiocyanate (FITC; Scheme S3, ESI†) and administered orally in a mouse model. Near-infrared fluorescence images showed that the polymer was distributed mainly in the intestine (99.6%) at 1 h and in the feces (90.1%) at 24 h after administration, as indicated by the excised organs (Fig. 6). No distribution in the heart, liver, spleen, lung, or kidney was observed at either time point. Despite the weak adhesive capability of polyMECA, we observed no long-term retention of this material (only a little residue observed in the intestine at 24 h) or consequent intestinal obstruction. Moreover, in an *in vitro* 24 h degradation test, only 4.96 mg formaldehyde was generated (corresponding to 0.2% polyMECA degradation, according to the reversed Knoevenagel approach[42]). The contribution of the formaldehyde pathway to the degradation of polyMECA was surprisingly poor, due to its limitation in water and at physiological pH. Hydrolysis

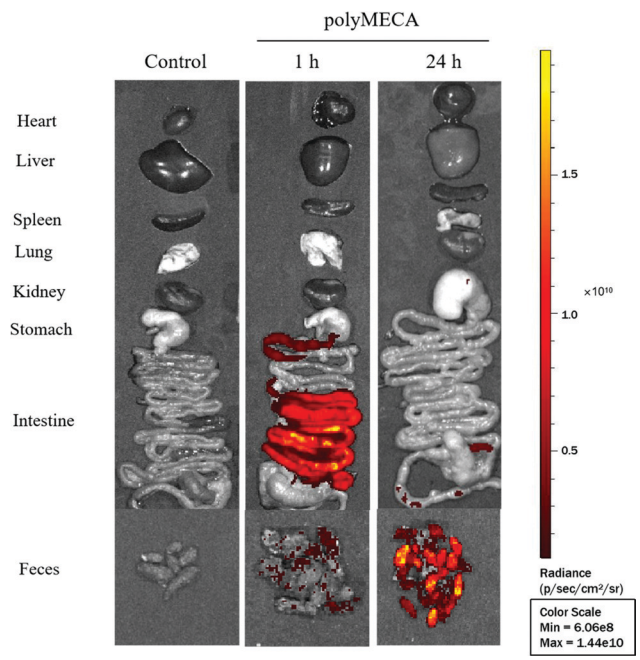

Fig. 6 Representative *ex vivo* fluorescence images of the dissected organs of mice given polyMECA by oral gavage and sacrificed 1 and 24 h thereafter.

of the ester function is another degradation route (Fig. S8, ESI†). This was confirmed by the estimation of the acid produced by the ester hydrolysis. The consumption of sodium hydroxide corresponded to the limited hydrolysis of the ester bond (1.07%). These results, which are consistent with the GPC analysis, not only indicate the hurdle of the degradation of the polymer, but also suggest the restricted absorption of orally administered polyMECA.

Anti-atherosclerosis treatment effect of ASA–polyMECA–HPMCP

The anti-atherosclerosis effect of ASA–polyMECA–HPMCP was evaluated in a rabbit model [Fig. 7(a)]. After treatment, aortas from the heart to the iliac bifurcation were stained with Oil-Red-O (ORO). *En face* aorta images and the quantification of lesion area revealed atherosclerotic lesions with typical post-modeling features in the control group, and significantly delayed plaque development in the aortic arch and thoracic aorta in the ASA–polyMECA–HPMCP group relative to the controls [Fig. 7(b) and (c)]. Average plaque areas in ORO-stained samples were 21.47% ± 2.12% in the ASA–polyMECA–HPMCP group and 47.76% ± 4.15% in the control group.

As the rupture of vulnerable plaques may lead to fatal complications,[43] we histopathologically examined the stability of atherosclerotic plaques after treatment. Masson's trichrome staining revealed that the content of collagen surrounding plaques was enhanced considerably, resulting in thicker fibrous caps, after treatment with ASA–polyMECA–HPMCP [Fig. 7(d) and (e)]. Immunohistochemical analysis revealed a reduced level of matrix metalloproteinase (MMP)-9, which can contribute to the development of vulnerable plaques,[44] in aortas [Fig. 7(f) and (g)]. Taken together, these results suggest that ASA–polyMECA–HPMCP exerted good anti-atherogenic effects without increasing plaque vulnerability.

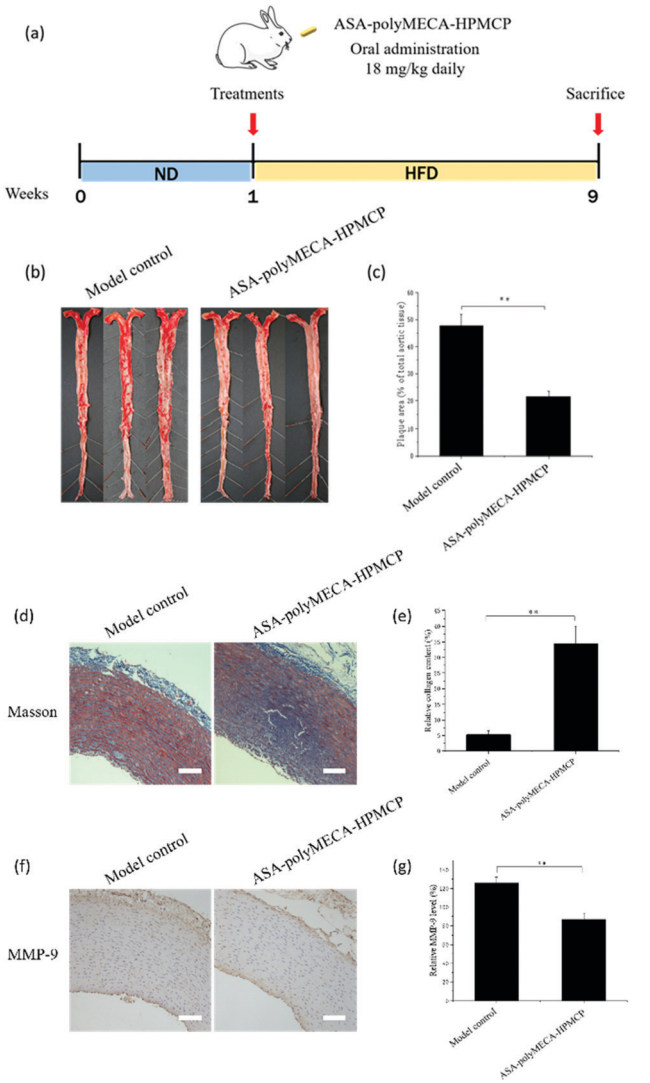

Fig. 7 Treatment of atherosclerosis with ASA–polyMECA–HPMCP in New Zealand white rabbits. (a) Time course of the experiment. Saline, ASA–polyMECA–HPMCP (18 mg kg^{-1} ASA) was administered orally once a day after 1 week of ND. (b) Representative photographs of *en face* ORO-stained aortas from each group. (c) Areas of lesions in (b). (d) Representative histological images of aortic root sections after Masson staining. ×100 magnification. The scale bar is 200 μm. (e) Quantification of the collagen content in (d). (f) Sections stained with antibodies to MMP-9. ×100 magnification. The scale bar is 200 μm. (g) MMP-9 levels. Data are means ± SDs. $^{**}p < 0.01$.

ASA–polyMECA–HPMCP prevents ASA irritation of the gastric mucosa

In our formulations, the HPMCP coating and polyMECA depot were meant to prevent ASA degradation and burst release in the stomach, thereby preventing irritation of the gastric mucosa. In the rabbit study of atherosclerosis treatment, rabbits given ASA–polyMECA–HPMCP showed no gastric bleeding or histomorphological abnormality, indicating good biocompatibility,

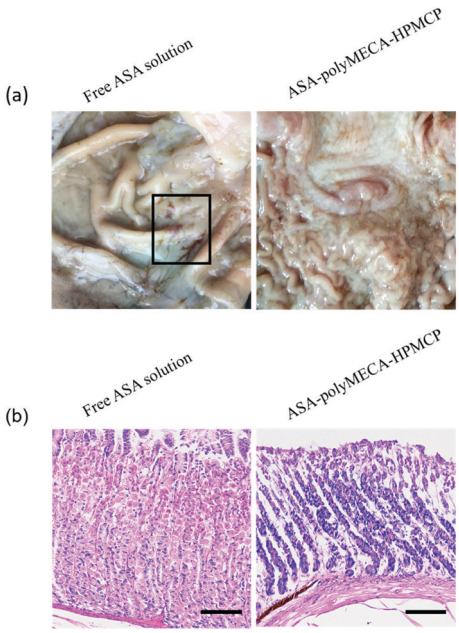

Fig. 8 Protective effect of ASA–polyMECA–HPMCP against ASA-induced bleeding in the stomach. (a) Representative images of the gastric mucosa, showing damage in rabbits given free ASA solution. (b) Representative histomorphological images of the gastric mucosal layer, showing ulceration induced by ASA. ×100 magnification. The scale bar is 200 μm.

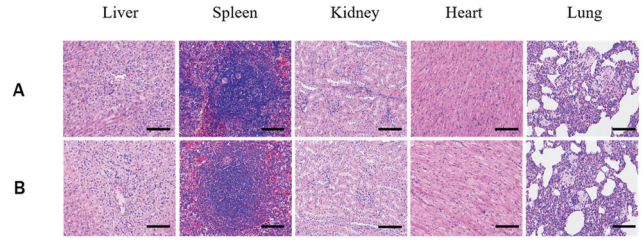

Fig. 9 H&E-stained histological sections of the heart, liver, spleen, and kidneys of (A) normal group and (B) ASA–polyMECA–HPMCP group at 9 weeks after treatment initiation. The images were obtained using a Leica microscope. ×200 magnification. The scale bar is 100 μm.

whereas those given free ASA solution (control) showed mucosal damage and even perforation in the glandular region of the stomach, resulting in the death of all animals within 6 days after treatment initiation [Fig. 8(a)]. Microscopic examination of the gastric mucosa of rabbits in the control group revealed the occurrence of epithelial erosion, the separation and exfoliation of cells lining the gastric pit, the presence of inflammatory infiltrates, and the suffusion of blood into the mucosa [Fig. 8(b)].

ASA–polyMECA–HPMCP showed low systemic toxicity

Compared with the normal group, rabbits treated with ASA–polyMECA–HPMCP in the *in vivo* atherosclerosis experiment showed no pathological alteration or toxicity in the liver, spleen, kidneys, heart, or lungs (Fig. 9). Thus, the ASA–polyMECA–HPMCP sample and the novel CA-based matrix excipient did not induce inflammation in tissues and was very safe at the dosage used.

Safety of polyMECA

The safety of polyMECA, a novel drug-loading depot ingredient, was further evaluated in acute and subchronic toxicity studies.

No acute toxicity was observed for polyMECA, even at 2.5 g kg^{-1} (orally administered), in a mouse model. No death or hazardous sign of toxicity was recorded during the 14 day observation period. Increases in body weight over time were similar in polyMECA-treated and control [0.5% (wt%) hypromellose aqueous solution (CMC)-fed] mice (Fig. S9, ESI†). Upon sacrifice at 14 days,

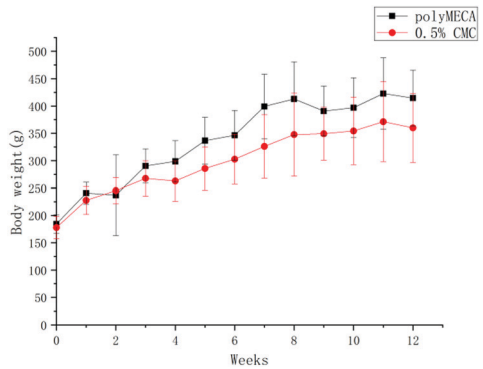

Fig. 10 Body weights of rats treated with polyMECA and CMC. Data are means ± SDs (n = 5).

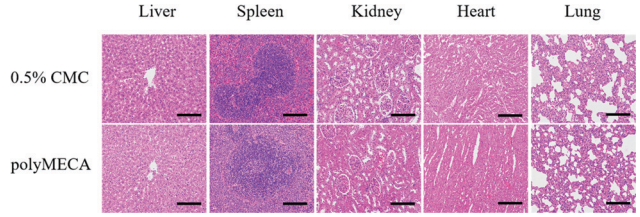

Fig. 11 Histopathological sections of major organs after the 90 day repeated dose toxicity assessment. ×200 magnification. The scale bar is 100 μm.

Table 3 Effects of the subchronic 12 week oral administration of polyMECA or 0.5% CMC on hematological parameters in SD rats

Hematological parameter	0.5% CMC	PolyMECA	p values
WBC (10^9 L^{-1})	7.63 ± 1.76	8.73 ± 1.27	0.43
RBC (10^{12} L^{-1})	7.91 ± 0.79	8.72 ± 1.50	0.46
HGB (g L^{-1})	141.00 ± 10.82	145.33 ± 8.50	0.61
PLT (10^9 L^{-1})	909.00 ± 119.15	951.67 ± 150.13	0.72
GRAN (10^9 L^{-1})	0.93 ± 0.25	1.10 ± 0.26	0.47
LYM (10^9 L^{-1})	6.53 ± 1.70	7.43 ± 0.92	0.47
MID (10^9 L^{-1})	0.17 ± 0.06	0.20 ± 0.10	0.64

Table 4 Effects of the subchronic 12 week oral administration of polyMECA or 0.5% CMC on biochemical parameters in SD rats

Biochemical parameter	0.5% CMC	PolyMECA	p values
ALT (U L^{-1})	77.38 ± 13.22	87.92 ± 10.90	0.43
AST (U L^{-1})	148.90 ± 36.81	146.35 ± 9.99	0.93
BUN (mg dL^{-1})	23.02 ± 1.61	21.40 ± 3.55	0.59
Cr (μmol L^{-1})	53.87 ± 5.44	50.73 ± 11.59	0.75

pathological examination revealed no abnormality in any major organ (Fig. S10, ESI†).

In the subchronic toxicity test, daily oral administration of 0.25 g kg^{-1} polyMECA for 12 weeks resulted in no treatment-related mortality or clinical sign of general toxicity. Body weight, the external physical structure of the organs, hematological parameters, and serum biochemistry profiles did not differ between polyMECA-treated and control rats (Fig. 10, 11 and Tables 3, 4).

Taken together, these results demonstrate the good biological safety of orally administered polyMECA and ASA–polyMECA–HPMCP *in vivo*.

Conclusions

A novel sustained intestinal drug delivery system featuring polyMECA excipient filling in an HPMCP capsule was developed in this work. The HPMCP acted as the protective shell for intestinal targeting. The liquid MECA can directly dissolve ASA, and the liquid–solid transformational property endows easy molding into desired shape and doses. Alkoxy modification of the CA matrix provided a suitable drug release rate and appropriate bioadhesive capability, resulting in improved

bioavailability of ASA loaded in an ASA–polyMECA–HPMCP formulation. ASA–polyMECA–HPMCP had desirable anti-atherosclerotic effects in a rabbit model. The novel medicinal adjuvant polyMECA was excreted completely in feces after drug release, and showed good biological safety. Thus, this work resulted in the development of a novel ITODD system with improved drug absorption efficiency. In addition to ASA delivery, it has potential broad applicability, such as in the treatment of enteritis and intestinal cancer.

Experimental

Chemicals

ASA and SA were obtained from InnoChem Chemical Reagent Beijing Co., Ltd (Beijing, China). All other chemicals, reagents, and solvents used in this work were purchased from Sinopharm Chemical Reagent Beijing Co., Ltd (Beijing, China). All solutions were prepared with deionized water produced by a Milli-Q Advantage water purification system (Millipore, USA). Soluble ECs made of HPMCP were obtained from Shaoxing Kangke Capsule Co., Ltd (Zhejiang, China). ASA-ECs were obtained from Yung Shin Pharm. Ind. (Kunshan) Co., Ltd (Jiangsu, China). ASA-ETs were obtained from Bayer (China).

Animals and ethical approval

Animals were purchased from the Beijing Experimental Animal Center (Beijing, China). All animal care and experiments were performed according to the Care and Use of Laboratory Animals guidelines of the Institute of Laboratory Animal Resources of the National Research Council (USA). The *in vivo* experiment was performed at the State Key Laboratory of Toxicology and Medical Countermeasures, Beijing Institute of Pharmacology and Toxicology, and approved by the institute's Animal Care and Use Committee. Best efforts were made to minimize the number of animals used and their suffering.

Monomer synthesis

BCA and MECA were synthesized using conventional methods (Schemes S1 and S2, ESI†). The total productivity was 52.3% for BCA and 46.5% for MECA. Their chemical structures were confirmed by ^{1}H-NMR (JNM-ECA-400; JEOL, Japan); $CDCl_3$ was used as the solvent. The purity was confirmed by gas chromatography (GC2010 PLUS; Shimadzu, Japan).

ASA–polyCA–HPMCP complex preparation

The ASA and liquid CA monomers were mixed at a certain weight ratio in a vortex mixer to yield a clear and transparent liquid state at room temperature. An appropriate amount (5%, ASA in CA) of drug-loading liquid was poured into the HPMCP capsule, which was then stored at 80 °C for 24 h until the CA matrix excipients had polymerized completely and solidified, yielding the final ASA–CA–HPMCP complex.

Estimation of drug release from ASA–polyCA–HPMCP capsules *in vitro*

The profile of ASA release from the ASA–polyCA–HPMCP complex was investigated using an HPLC device (C-10AT; Shimadzu, Japan) equipped with a Diamonsil C-18 column (4.6 × 250 mm, 5 μm particle size; Dikma, China). The ASA–polyCA–HPMCP complexes were immersed successively in buffer solutions simulating gastric fluid (pH 1.2) and intestinal fluid (pH 6.8). The dissolution media were maintained at 37 °C and stirred at 100 rpm. Samples (500 μL) were withdrawn at predetermined time points (n = 3) and the media were replaced. The samples were injected into the injector port of the HPLC device and analyzed at 266 nm; the mobile phase used was acetonitrile:acetic acid:tetrahydrofuran:water at a ratio of 20 : 5 : 5 : 70 and a flow rate of 1 mL min^{-1}.

Drug distribution in the ASA–polyMECA complex

$CDCl_3$ was used as the solvent for ^{1}H-NMR analysis. The UV absorbance of ASA–polyMECA at 200–350 nm was measured in methyl alcohol using a Cary-100 Bio UV-visible spectrophotometer (Varian) and a standard scanning program. HPLC was performed as described in the previous section.

In vitro release of ASA from ASA–polyMECA–HPMCP

The *in vitro* release of ASA from ASA–polyMECA–HPMCP was measured in triplicate using the method described in the Estimation of drug release from ASA–polyCA–HPMCP capsules *in vitro* section. Commercially available ASA-ECs and ASA-ETs served as positive controls. In addition, the release profiles of ASA–polyMECA–HPMCP with different drug loading rates (5%, 10%, and 15%, determined by quantificationally dissolving ASA in liquid MECA) and matrix volumes (50, 100, and 200 μL) in different media were investigated by the same method as in previous section.

In vivo analysis of ASA–polyMECA–HPMCP pharmacokinetics

For the pharmacokinetic analysis, male New Zealand white rabbits with a mean body weight of 2 ± 0.2 kg (8 weeks) were divided randomly into four groups (n = 9/group) orally administered ASA–polyMECA–HPMCP with 18 mg kg^{-1} ASA, ASA–polyMECA–HPMCP with 24 mg kg^{-1} ASA, free ASA solution with 24 mg kg^{-1} ASA, and ASA-ECs with 24 mg kg^{-1} ASA, respectively. Before administration, the rabbits were fasted for 12 h, but had access to water. Blood samples were collected into heparinized tubes at different time points and centrifuged at 4000 rpm for 5 min. Plasma samples were stored at −20 °C before analysis. Salicylate was extracted from the plasma samples by vortexing 50 μL of plasma and 125 μL of 0.5% formic acid with two 500 μL aliquots of methyl *tert*-butyl ether (MTBE). The MTBE layers were combined, evaporated to dryness, and reconstituted in 200 μL of the HPLC mobile phase for analysis. The HPLC conditions were the same as in the Estimation of drug release from ASA–polyCA–HPMCP capsules *in vitro* section.

GPC analysis

GPC was performed with a Waters 1515 system (Waters, USA) to determine the molecular weight of polyMECA. The polymers (25 mg) were dissolved in tetrahydrofuran (THF, 0.5 mL), and then refiltered through syringe filters with 0.22 μm aperture before analysis. The experiments were repeated at least three times.

Assessment of the metabolism and distribution of orally administered polyMECA in mice

An FITC-labeled CA monomer 6-amino-1-hexanol cyanoacrylate was synthesized using conventional methods (Scheme S3, ESI†), then mixed and copolymerized with MECA (97%, wt%). A suspension of the copolymer powder (20%) in 0.5% carboxymethyl cellulose (CMC) solution was prepared for intragastric administration (2.5 g kg^{-1}) in Kunming mice (male, 20 ± 2 g, n = 3). Normal saline is used as the control. The animals were placed in individual metabolism chambers immediately after dosing with the FITC-labeled copolymer, then sacrificed at 1 and 24 h, respectively. The stomach, small intestine, colon, heart, liver, spleen, lungs, kidneys, and feces were collected. Fluorescent images of the excreta and major organs were acquired using an IVIS SPECTRUM *in vivo* imaging system (PerkinElmer, UK) for the observation of polyMECA metabolism and distribution.

Rabbit model of atherosclerosis treatment

Male white New Zealand rabbits (n = 16) weighing 2.0 ± 0.2 kg (8 weeks) were used for the atherosclerosis treatment model. The rabbits were fed with ND for 1 week, and then HFD containing 0.5% cholesterol, 5% sucrose, and 5% lard for 8 weeks. They were divided randomly into two groups (n = 8 each) given normal saline (model control) and ASA–polyMECA–HPMCP (drug efficiency is 15%) orally daily from week 2.

At the end of the treatment period, the rabbits were euthanized. The degree of pathological changes was evaluated by measuring the lesion (plaque) area on the aorta from the heart to the iliac bifurcation. The aorta was fixed with 10% neutral formaldehyde, the periadventitial tissue was cleaned, and the aorta was opened longitudinally and stained with ORO. To determine the stability of atherosclerotic plaques at the aortic root, the aortic sinus was fixed in 10% formalin for 50 min, then embedded in paraffin and cut into 6 mm sections. The sections were stained with Masson stain to quantify the content of collagen. In addition, overnight incubation with antibodies to matrix metalloproteinase-9 (MMP-9) was performed for MMP-9 quantification. The histological and immunohistochemical analyses were performed with a Panoramic 250 device (3D HISTECH, Hungary).

Side effect evaluation

Following 2 months of atherosclerosis treatment *in vivo*, the liver, spleen, lungs, kidneys, and heart of rabbits were sampled to study the histotoxicity of ASA–polyCA–HPMCP. For the examination of gastric mucosal damage, the stomach was excised and opened along the greater curvature. 18 mg kg^{-1} of free ASA solution is used as the control. Gastric lesions were photographed with a camera. Histological examination of the stomach samples was also performed. The photographs of the gastric lesions were taken with a photomicroscope.

Acute oral toxicity assessment

Ten healthy male Kunming mice (20 ± 2 g) were divided randomly into two groups (n = 5 each). The animals were fasted overnight, but had free access to water. They were weighed before oral administration of 0.5% CMC aqueous solution (control) or a limit dose of the 0.5% CMC suspension containing 20% MECA prepolymer powder (2.5 g kg^{-1}). Food was withheld for an additional 3–4 h after treatment. The animals were observed individually to detect changes in general behavior and body weight, toxic symptoms, and mortality periodically for the first 24 h and daily thereafter for 14 days. At the end of the experimental period, all animals were weighed and sacrificed by cervical dislocation, and the organs were removed for necropsy.

Twelve-week subchronic toxicity study

According to the acute toxicity study results, the subchronic toxicity dose was set at 0.25 g kg^{-1}. Twenty rats of both sexes (180 ± 10 g) were divided into two groups [n = 10 (5 males and 5 females)/group] and their weights were recorded. The control group was given 0.5% CMC aqueous solution and the polyMECA group was given 0.5% CMC suspension containing 20% MECA prepolymer powder (0.25 g per kg body weight per day) by oral gavage for 12 weeks. The body weight and food and water intake were recorded weekly. At the end of the study period, the rats were sacrificed by cervical dislocation and blood samples were taken by retro-orbital puncture using EDTA capillary tubes for hematological and biochemical studies. The liver, kidneys, spleen, lungs, and heart were collected, washed immediately in NaCl (0.9%), and examined macroscopically. Hematological analysis of blood samples was performed using an automated hematology analyzer (Mindrary BC-2800vet, China). Biochemical parameters were estimated using a Rayto Chemray 800 automated biochemical analyzer (China). Histopathological analysis of the preserved organs and tissues was performed. Photomicrographs were taken using a NIKON DS-F12 digital sight imaging system (Nikon Corporation, Tokyo, Japan).

Statistical analysis

The data were analyzed using two-tailed Student's t tests. P values < 0.05 were considered to be significant.

Conflicts of interest

The authors have no conflict of interest to declare.

Acknowledgements

Financial support from the Beijing Natural Science Foundation (7202146) is gratefully appreciated.

References

1 L. H. Nielsen, S. S. Keller and A. Boisen, *Lab Chip*, 2018, **18**, 2348–2358.
2 F. Hallouard, L. Mehenni, M. Lahiani-Skiba, Y. Anouar and M. Skiba, *Curr. Pharm. Des.*, 2016, **22**, 4942–4958.
3 J. E. Vela Ramirez, L. A. Sharpe and N. A. Peppas, *Adv. Drug Delivery Rev.*, 2017, **114**, 116–131.
4 W. Fan, D. Xia, Q. Zhu, X. Li, S. He, C. Zhu, S. Guo, L. Hovgaard, M. Yang and Y. Gan, *Biomaterials*, 2018, **151**, 13–23.
5 C. Yang, Y. Zhang, P. Cai, S. Yuan, Q. Ma, Y. Song, H. Wei, Z. Wu, Z. Wu and X. Qi, *J. Drug Targeting*, 2020, **28**, 102–110.
6 N. Reix, P. Guhmann, W. Bietiger, M. Pinget, N. Jeandidier and S. Sigrist, *Int. J. Pharm.*, 2012, **422**, 338–340.
7 M. Mabrouk, J. A. Mulla, P. Kumar, D. R. Chejara, R. V. Badhe, Y. E. Choonara, L. C. du Toit and V. Pillay, *AAPS PharmSciTech*, 2016, **17**, 1120–1130.
8 E. Antonelli, V. Villanacci and G. Bassotti, *World J. Gastroenterol.*, 2018, **24**, 5322–5330.
9 J. Hu, Y. Sheng, J. Shi, B. Yu, Z. Yu and G. Liao, *Curr. Drug Metab.*, 2018, **19**, 723–738.
10 A. Mandal, R. Bisht, I. D. Rupenthal and A. K. Mitra, *J. Controlled Release*, 2017, **248**, 96–116.
11 Q. Zhou, L. Zhang, T. Yang and H. Wu, *Int. J. Nanomed.*, 2018, **13**, 2921–2942.
12 F. Guo, T. Ouyang, T. Peng, X. Zhang, B. Xie, X. Yang, D. Liang and H. Zhong, *Biomater. Sci.*, 2019, **7**, 1493–1506.
13 T. Woraphatphadung, W. Sajomsang, T. Rojanarata, T. Ngawhirunpat, P. Tonglairoum and P. Opanasopit, *AAPS PharmSciTech*, 2018, **19**, 991–1000.
14 W. Zhang, K. M. Mahuta, B. A. Mikulski, J. N. Harvestine, J. Z. Crouse, J. C. Lee, M. G. Kaltchev and C. S. Tritt, *Pharm. Dev. Technol.*, 2016, **21**, 127–130.
15 Y. Karrout, C. Neut, D. Wils, F. Siepmann, L. Deremaux, L. Dubreuil, P. Desreumaux and J. Siepmann, *Eur. J. Pharm. Biopharm.*, 2009, **73**, 74–81.
16 Y. Dou, Y. Chen, X. Zhang, X. Xu, Y. Chen, J. Guo, D. Zhang, R. Wang, X. Li and J. Zhang, *Biomaterials*, 2017, **143**, 93–108.
17 G. K. Hansson, *N. Engl. J. Med.*, 2005, **352**, 1685–1695.
18 J. Moriya, *J. Cardiol.*, 2019, **73**, 22–27.
19 P. M. Ridker, *Trans. Am. Clin. Climatol. Assoc.*, 2013, **124**, 174–190.
20 P. M. Ridker, B. M. Everett, T. Thuren, J. G. MacFadyen, W. H. Chang, C. Ballantyne, F. Fonseca, J. Nicolau, W. Koenig, S. D. Anker, J. J. P. Kastelein, J. H. Cornel, P. Pais, D. Pella, J. Genest, R. Cifkova, A. Lorenzatti, T. Forster, Z. Kobalava, L. Vida-Simiti, M. Flather, H. Shimokawa, H. Ogawa, M. Dellborg, P. R. F. Rossi, R. P. T. Troquay, P. Libby and R. J. Glynn, *N. Engl. J. Med.*, 2017, **377**, 1119–1131.
21 P. Libby, *Arterioscler., Thromb., Vasc. Biol.*, 2012, **32**, 2045–2051.
22 U. Hedin and L. P. Matic, *J. Vasc. Surg.*, 2019, **69**, 944–951.
23 B. K. Martinez and C. M. White, *Ann. Pharmacother.*, 2018, **52**, 801–809.
24 M. E. Tsoumani, K. I. Kalantzi, I. A. Goudevenos and A. D. Tselepis, *Curr. Vasc. Pharmacol.*, 2012, **10**, 539–549.
25 C. H. Hennekens, O. Sechenova, D. Hollar and V. L. Serebruany, *J. Cardiovasc. Pharmacol. Ther.*, 2006, **11**, 170–176.
26 R. De Caterina, E. D'Ugo and P. Libby, *Thromb. Haemostasis.*, 2016, **116**, 1012–1021.
27 L. Zhang, T. Li, X. Miao, L. Ding, S. Wang and Y. Wang, *BioFactors*, 2019, **45**, 343–354.
28 D. A. Chistiakov, A. A. Melnichenko, A. V. Grechko, V. A. Myasoedova and A. N. Orekhov, *Exp. Mol. Pathol.*, 2018, **104**, 114–124.
29 C. J. Lavie, C. W. Howden, J. Scheiman and J. Tursi, *Curr. Probl. Cardiol.*, 2017, **42**, 146–164.
30 I. B. Richman and D. K. Owens, *Med. Clin. North Am.*, 2017, **101**, 713–724.
31 P. Terrosu, *Monaldi. Arch. Chest. Dis.*, 2016, **84**, 728.
32 F. F. Sahle, C. Gerecke, B. Kleuser and R. Bodmeier, *Int. J. Pharm.*, 2017, **516**, 21–31.
33 B. Singh, S. Maharjan, T. Jiang, S. K. Kang, Y. J. Choi and C. S. Cho, *Biomaterials*, 2015, **59**, 144–159.
34 J. M. Korde and B. Kandasubramanian, *Biomater. Sci.*, 2018, **6**, 1691–1711.
35 S. Mura, E. Fattal and J. Nicolas, *J. Drug Targeting*, 2019, **27**, 470–501.
36 D. R. Janagam, L. Wu and T. L. Lowe, *Adv. Drug Delivery Rev.*, 2017, **122**, 31–64.
37 T. Zhang, Y. Tang, W. Zhang, S. Liu, Y. Zhao, W. Wang, J. Wang, L. Xu and K. Liu, *J. Mater. Chem. B*, 2018, **6**, 1216–1225.
38 H. Stevens, M. Voelker, L. Gow, F. Macdougall and G. Bieri, *J. Drug Delivery Sci. Technol.*, 2019, **51**, 535–541.
39 Y. Wang, P. P. Xu, X. X. Li, K. Nie, M. F. Tuo, B. Kong and J. Chen, *J. Pharm. Anal.*, 2012, **2**, 386–389.
40 J. Xu, S. Strandman, J. X. Zhu, J. Barralet and M. Cerruti, *Biomaterials*, 2015, **37**, 395–404.
41 M. Alibolandi, F. Alabdollah, F. Sadeghi, M. Mohammadi, K. Abnous, M. Ramezani and F. Hadizadeh, *J. Controlled Release*, 2016, **227**, 58–70.
42 H. Dae, S. Park, K. Bum, A. Kwang-Duk and E. Yong, *J. Appl. Polym. Sci.*, 2003, **89**, 3272–3278.
43 K. Kobiyama and K. Ley, *Circ. Res.*, 2018, **123**, 1118–1120.
44 W. Eilenberg, S. Stojkovic, A. Kaider, N. Kozakowski, C. M. Domenig, C. Burghuber, J. Nanobachvili, K. Huber, M. Klinger, C. Neumayer, I. Huk, J. Wojta and S. Demyanets, *Clin. Chem. Lab. Med.*, 2017, **56**, 147–156.

